Supplement of Solid Earth, 14, 499–514, 2023
https://doi.org/10.5194/se-14-499-2023-supplement

Solid Earth
Open Access

Supplement of

Mapping the basement of the Cerdanya Basin (eastern Pyrenees) using seismic ambient noise

Jordi Díaz et al.

Correspondence to: Jordi Díaz (jdiaz@geo3bcn.csic.es)

Supplemental Materials

Supplementary Material S1: Details of the RFs calculation

In order to obtain the RFs presented in this contribution, we have followed a classical approach, already used in a prior RFs study in the eastern Pyrenees published by the same author team (Diaz el at., 2018).
The first step in data processing was to select teleseismic events with magnitude higher than 5.5, epicentral distances between 35º and 95º and clear P arrivals. We then calculated the corresponding RF by frequency domain deconvolution (Langston, 1979) of the vertical component from the horizontal components in the time window corresponding to the P arrival and its coda. Prior to the RF calculation, data has been high-pass filtered with a corner frequency of 0.1 Hz to avoid problems due to low-frequency signals. The deconvolution was performed using the classical "pwaveqn" software (Ammon, 1997), using a value of 10 for the low-pass gaussian filter parameter, equivalent to pulse width around 0.5 s, to preserve the high frequency content of the signals and hence allow a better delineation of the crustal discontinuities. A standard value of 0.05 is used as water level parameter to avoid numerical problems during deconvolution. An automatic workflow has been implemented to calculate RFs, retaining only those signals with large signal-to-noise ratio of the incoming phases. In a second step, the selected events have been visually inspected in order to discard unclear records. The number of finally retained events ranges between 22 and 57, with a mean value of 46 retained RFs per station.

The traces shown in Figure 3 are obtained by applying Ps-moveout correction to a reference ray parameter of 0.065 s/km to the selected RFs and sum the corrected traces for each of the stations located along the Cerdanya Basin.

References:

Ammon, C.J., 1997. An overview of receiver function analysis. http://eqseis.geosc.psu.edu/~cammon/HTML/RftnDocs/rftn01.html.

Diaz, J., Vergés, J., Chevrot, S., Antonio-Vigil, A., Ruiz, M., Sylvander, M., Gallart, J., 2018. Mapping the crustal structure beneath the eastern Pyrenees. Tectonophysics. https://doi.org/10.1016/j.tecto.2018.07.011.

Langston,C.A., 1979. Structure under Mount Rainier, Washington, inferred from teleseismic body waves. J. Geophys. Res., 84, 4749-4762.

Supplementary Material S2: Representative H/V measurements at broad-band stations (left panels) and seismic nodes (right panels).

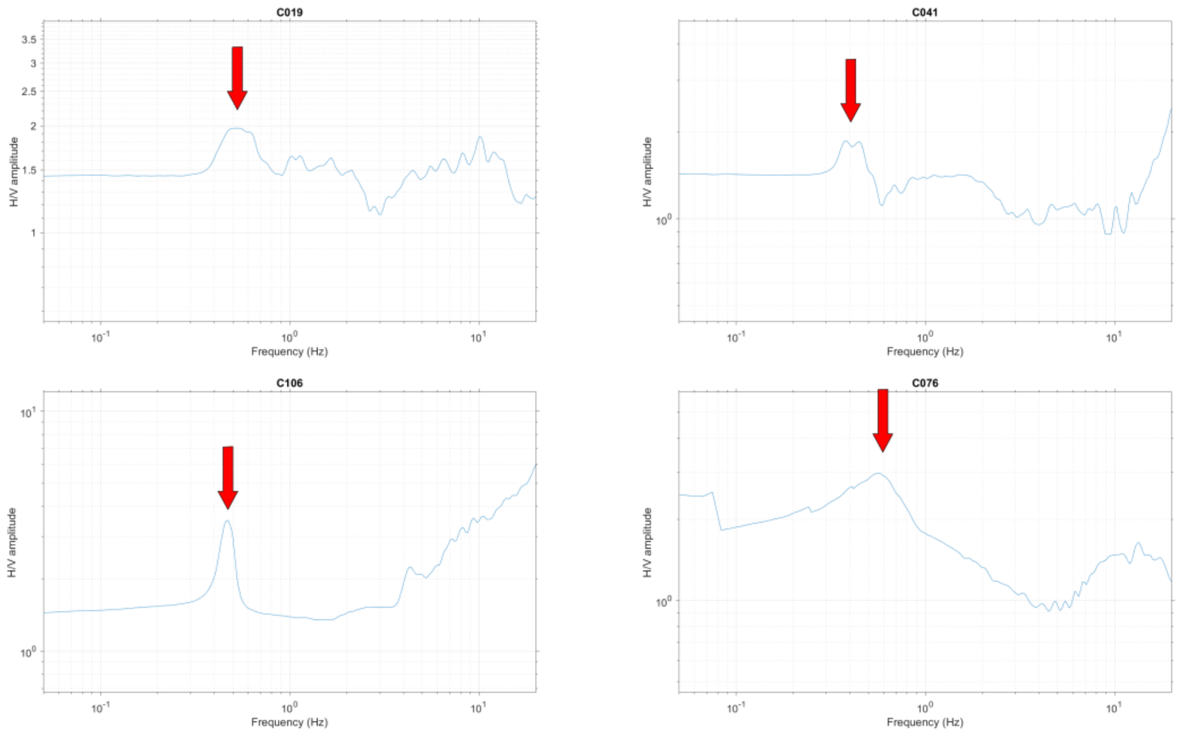

Supplementary Material S3: Seismic noise amplitude calibration. a) Correlation between the basement depth estimations from Gabàs et al. 2016 (squares) and seismic power amplitudes measured in our dataset (circles). Color palettes have been chosen to visualize the correlation between both datasets. Backgroung shading represents topography. b) Adjustment between seismic noise amplitudes and basement depths. Blue line shows the degree 2 polynomial adjustment.

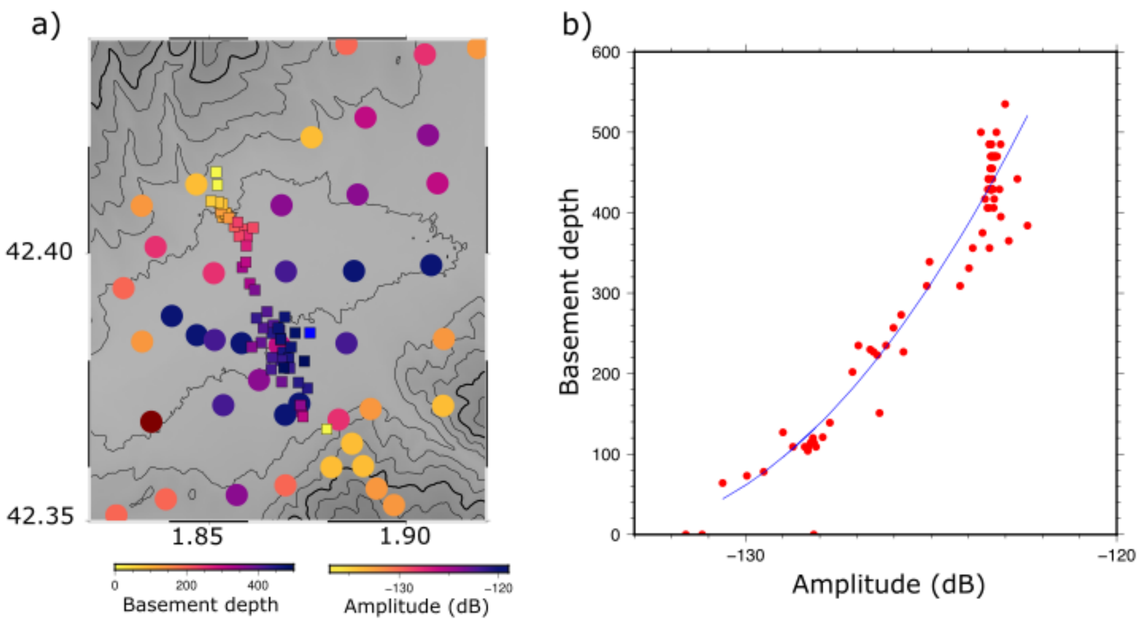

Supplementary Material S4: Comparison of the basement depths retrieved from different methods.

Basement depths estimations from Gabas et al (2016) (black dots) compared with the values extracted from the HVSR dataset (blue circles) and seismic noise amplitude (red circles). The inset map shows the basement depth estimations of the Gabas et al (2016) profile and can be compared with the results of our study (Fig. 9b)